Check for
updates

Flood Modeling and Prediction Using Earth Observation Data

Guy Schumann[1,2] · Laura Giustarini[1] · Angelica Tarpanelli[3] · Ben Jarihani[4,5] ·
Sandro Martinis[6]

Abstract
The ability to map floods from satellites has been known for over 40 years. Early images of floods were rather difficult to obtain, and flood mapping from satellites was thus rather opportunistic and limited to only a few case studies. However, over the last decade, with a proliferation of open-access EO data, there has been much progress in the development of Earth Observation products and services tailored to various end-user needs, as well as its integration with flood modeling and prediction efforts. This article provides an overview of the use of satellite remote sensing of floods and outlines recent advances in its application for flood mapping, monitoring and its integration with flood models. Strengths and limitations are discussed throughput, and the article concludes by looking at new developments.

Keywords Earth Observation · Floods · Flood mapping · Data assimilation · Flood Modeling

Article Highlights

- Synthetic Aperture Radar satellite imagery can be used to map urban flooding
- Satellite data on floods can help improve flood forecasting models
- Satellite images of floods can inform better flood disaster response and management

✉ Guy Schumann
gjpschumann@gmail.com

1   Research and Education Department (RED), RSS-Hydro, L-3593 Dudelange, Luxembourg

2   School of Geographical Sciences, University of Bristol, Bristol BS8 1SS, UK

3   Research Institute for Geo-Hydrological Protection, National Research Council, 06128 Perugia, Italy

4   Earth and Environmental Sciences, University of Central Asia, 720001 Tajikistan, Kazakhstan

5   University of the Sunshine Coast, Sunshine Coast, QLD 4556, Australia

6   German Aerospace Center (DLR), German Remote Sensing Data Center (DFD), 82234 Oberpfaffenhofen, Germany

1 Introduction

Floods are most often a natural process by which water overtops its channels and inundates adjacent floodplain lands thereby sustaining habitats, livelihoods and ecosystem services. In fact, in many regions of the world such as in wetlands, coastal and inland delta systems (e.g., in the Amazon, Nile and Niger) floods are required to sustain food production and biodiversity. However, anomalous flooding can be devastating, causing fatalities and high socio-economic losses at local, regional, national and international levels. In 2017, in the span of just four weeks, the hurricane trio of Harvey, Irma and Maria made the hurricane season in the North Atlantic the costliest ever according to Munich Re (2017), one of the largest global re-insurers. In fact, for this devastating season alone, Munich Re reported overall losses to have reached around US \$220 bn and insured losses almost US \$90 bn. More recent, disastrous events, such as the European summer floods of July 2021 that have been attributed by science and industry to the effects of climatic change (Munich Re 2022) and have caused over 200 deaths (Copernicus 2021). Swiss Re, another global re-insurer, estimated total insured market losses of the insurance industry due to the July floods in Europe at approximately US \$12 bn (Insurance Journal 2021).

According to Swiss Re Institute's research, small- to mid-sized severe weather events, or secondary perils, accounted for more than 70% of insured losses from natural catastrophes in 2020, with precipitation-driven floods dominating secondary perils losses in Asia Pacific over the past decade (Swiss Re 2021).

Damaging flood events like these, and there have been many of this type in recent years, are very difficult to predict, respond to and, indeed, recover from. One main reason for this very challenging situation is that floods from hurricanes and tropical storms cover spatial and temporal scales that far exceed those covered by traditional monitoring and modeling tools, which are often observing at a point location or predict floods often only at reach scale.

In recent years though, significant advances in numerical modeling, data processing algorithms and the Internet of Things (IoT), in addition to a general proliferation of available data sets from remote sensing [Schumann and Domeneghetti 2016], have led to an application readiness level in products and services. The latter are now becoming mature enough so that new technologies can effectively assist flood disaster response teams and flood risk management (see Fig. 1 for an example in insurance applications) and resilience planning. Of course, this represents considerable progress but many challenges remain and many promising algorithms and tools are still in a development phase and are only slowly reaching truly operational capability.

There are many streams of information that can be available during a flood event and many complement each other while having their own strengths and limitations. On the one hand, models, run either for event forecasting or past event analysis or stochastically for uncertainty and risk assessments, typically have the obvious advantages to be continuous in time and can forecast flood inundation. However, models are inherently uncertain and often lack complete process representation or have inadequate, or low-resolution boundary data. On the other hand, remote sensing observations, in particular from satellites, cover large spatial scales at the desired resolutions but also suffer from large uncertainties, most often related to the Earth surface and atmospheric conditions, such as clouds, dense vegetation and buildings as well as topographic effects. It is now widely understood that much can be gained when integrating both model and satellite data of floods.
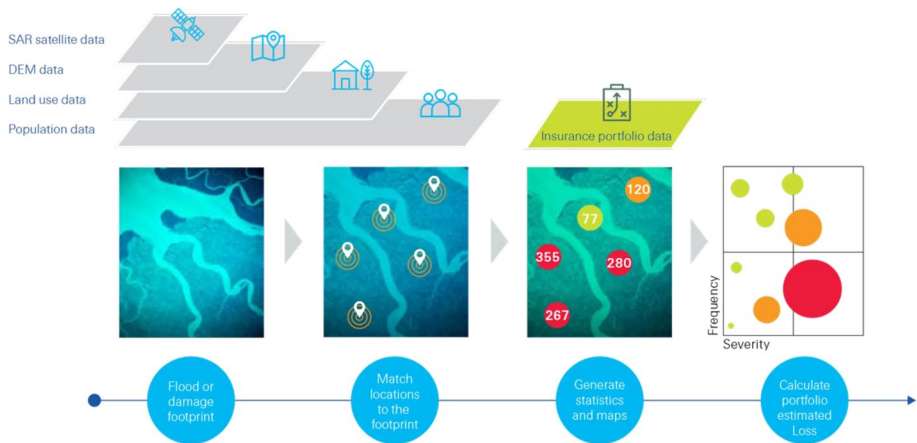
Fig. 1 Remote sensing data, where and when available, can be used to estimate flood extent, and the resultant output enriches the geo-referenced portfolio data to derive individual risk level damage estimates and helps obtain better insights on vulnerability curves for flood risk modeling (source: Swiss Re Institute)

Notwithstanding significant levels of uncertainties associated with Earth Observation data, the information that can be obtained from it can often overcome limitations of in situ measurements to monitor floods. Typical limitations of field-based data of floods include point-based observation, areas are difficult to access during floods, and high flows do typically not allow measurements to be collected. Furthermore, the global river gauge network is in decline due to high maintenance and operational costs.

This article will describe and discuss the various types of Earth Observation (EO) data typically used to monitor floods and describe methods to retrieve information on extent, water level, flood depth, and volume. Then, the article will describe and critically assess the various methods that exist to integrate EO data of floods with flood models while also discussing challenges. Finally, before concluding, the article will provide a brief outlook of possible future directions, including recent notable advances in machine learning methods.

2 Optical Imagery

If an image can be acquired, either by aircraft or satellite, in the visible to near-infrared range, then classifying water bodies and inundated areas is often more straightforward than on a radar image due to the fact that the human eye is more accustomed to this type of image and thus interpretation is easier.

Given the very high spatial resolution of aerial photography, flood extent is often derived from color or panchromatic aerial photography by simply digitizing the edges at the contrasting land–water interface. A very simple and straightforward approach to retrieving useful flood information from space consists of extracting a binary map consisting of dry and flooded pixels, most often in a fully- or semi-automated way. This procedure is applied throughout the world by many research teams and engineering and consulting companies, as well as emergency response services, and governmental institutions. Probably the most common image processing algorithm applied to an optical image for separating water and dry land is the classification using the Normalized Difference Water Index

(NDWI), or versions thereof. This index uses the reflected near-infrared radiation and visible green light to enhance the presence of open water surfaces while eliminating the presence of soil and terrestrial vegetation features (McFeeters 1996).

The potential of optical satellite images for flood science and applications has been known for over 40 years. Several studies in the early 1970s demonstrated the value of optical satellite imagery to map the evolution of flooding from space and indicated strong application potential for such maps for a number of sectors (e.g., Currey 1977; Deutsch and Ruggles 1978; Robinove 1978).

There is thus far a very large historical archive of over 40 years of optical satellite images available worldwide. This continues to grow with more missions being added to existing series (e.g., NASA's Landsat) or growing constellations (e.g., ESA's Sentinel-2), as well as the rapidly expanding availability of high-resolution commercial optical imagery, provided by, e.g., Planet, Maxar, or Airbus, and even smaller private industry entities. Given the recent proliferation of optical satellite images, various spatial and temporal resolutions are now available, either as open-access data for NASA or the European Copernicus missions, or via paid services in the case of high-resolution commercial images.

Presently, the Moderate Resolution Imaging Spectrometer (MODIS) onboard NASA's Terra and Aqua satellites acquires images twice daily all around the globe. This offers a unique capability to monitor flood events and assist disaster response where and when possible. Despite the relatively low spatial resolution (250 m), persistent cloud cover and vegetation, as well as densely built areas that limit successful flood detection, NASA processes these images in near-real time (NRT) and provides flood maps (Fig. 2A) to a number of flood relief agencies (for further reference, see NASA's NRT Global Flood Mapping and the Dartmouth Flood Observatory).

NASA's Terra and Aqua satellites mentioned above are currently approaching their end of mission life. The continuation of the data and information that these satellites delivered for many years could be guaranteed by the Visible Infrared Imaging Radiometer Suite (VIIRS) instrument, one of the five major EO instruments onboard NOAA's Suomi-NPP and JPSS (Joint Polar Satellite System) satellites, which is essentially a continuation of NOAA's AVHRR legacy sensors. With a very large swath width of 3060 km, it provides full daily coverage of the Earth both during the day and at night.

Using NOAA's VIIRS and the coastal flooding caused by Hurricane Sandy as a test case, Li et al. (2018) presented an approach to estimate the extent of large-scale floods in an operational setting (Fig. 2B). The approach estimates the water fraction from VIIRS 375-m imager data by applying a mixed-pixel linear decomposition and a dynamic nearest neighbor search method. By using the reflectance characteristics of the VIIRS visible, near-infrared and shortwave infrared channels, the method dynamically searches the nearby land and water end-members. As an optional post-processing step, based on simple physical characterization of water spreading, the low-resolution flood map from VIIRS can be downscaled to a higher spatial resolution using a digital elevation model; in their case, the output was downscaled to a 30 m pixel spacing.

More recently, the same algorithm has also been applied to images from NOAA's GOES-R/ABI (Geostationary Operational Environmental Satellite-R/Advanced Baseline Imager). GOES-R/ABI scans the Earth surface of CONUS (Continental United States) every five minutes with a resolution of 0.5–2 km, which can provide many more opportunities for cloud-free acquisitions during a flood event. Merging flood maps from both the GOES-R/ABI and VIIRS in near real-time can add substantial value to the final map product being delivered to the flood response community. The delivery system currently in place is the Unidata AWIPS (https://www.unidata.ucar.edu/software/awips2), which is a
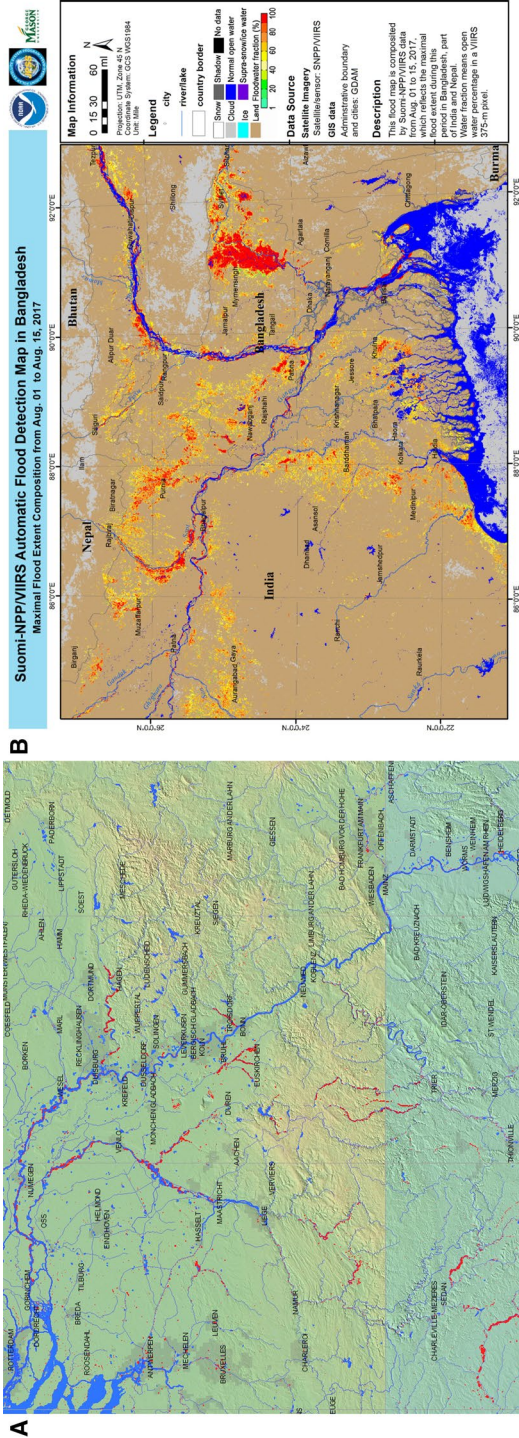
Fig. 2 A. European summer floods, 2021. Red is all flooding observed for this event. Mean annual flood and permanent water extent are blue and are above the red "flood" layer. Dark gray is all previously mapped flooding, since 1999. Light gray is a satellite-observed city lights layer. See also the DFO Web Map Server. Over the course of the event, remote sensing data are combined in red to show all flooded areas. Not all flooded areas may be observed due to cloud cover. Flood layers include: MODIS 250 m NRT from NASA GSFC, MODIS 250 m from DFO, NASA/JPL Aria System results using Sentinel-1 SAR, and flood mapping by the COPERNICUS Emergency Mapping Service (European Union) and ESA using Sentinel-1 SAR, Pleiades, and other sensors. Date range included in these maps: July 15–22, 2021. B. This flood map is composited by Suomi-NPP/VIIRS data from August 01 to 15, 2017, which reflects the maximal flood extent during this period in Bangladesh, part of India and Nepal. Water fraction means open water percentage in a VIIRS 375-m pixel

meteorological display and analysis package originally developed by the National Weather Service and Raytheon to support non-operational use in research and education by UCAR member institutions.

Notwithstanding the success of optical imagery for flood mapping (see Huang, C. et al. 2018; Marcus and Fonstad 2008) for a detailed scientific review), as noted earlier, the systematic application of such imagery is hampered by persistent cloud cover during floods, particularly in small to medium-sized basins where floods often recede before weather conditions improve, as is oftentimes the case in Europe for instance. Also, as already mentioned, the inability to map flooding in urban areas or beneath vegetation canopies, limits the applicability of optical sensors.

3 Synthetic Aperture Radar Imagery

Synthetic Aperture Radar (SAR) is one of the preferred sensors for flood mapping (see Shen et al. 2019 for a recent review) from space. A SAR sensor provides its own source of illumination in the microwave range. Therefore, it is characterized by near all-weather (high wind speed and intense precipitation cause problems), day-night imaging capabilities, independent of atmospheric conditions. This guarantees a continuous observation of the Earth surface and makes its preferred use for flood mapping obvious.

3.1 Open, Rural Areas

Smooth open water areas surfaces can be easily detected in SAR images. A flat water surface typically appears as dark homogeneous regions in SAR images, due to its specular reflection behavior. This causes relatively dark pixels in radar data which contrast with non-water areas (Fig. 3).

Visual interpretation is a simple method to derive flood maps from SAR images (Schumann et al. 2009). With this approach, contextual information can be taken into account; however, it risks being a rather time consuming task, and the final result strongly depends
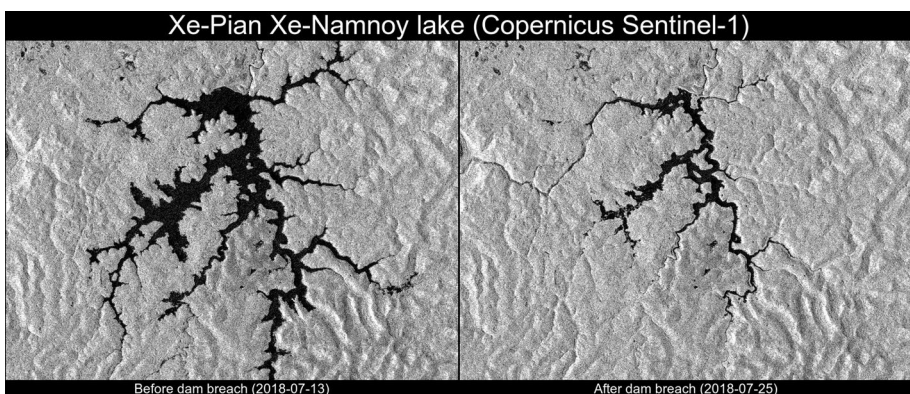

Fig. 3 Copernicus ESA's Sentinel-1 images show the impact of the dam failure on the Xe-Pian Xe-Namnoy lake area in the southeastern province of Attapeu in Laos. © Contains modified Copernicus Sentinel data (2018) / processed by CESBIO

on the ability of the image interpreter and result reproducibility is generally compromised (Martinis 2010).

Semi-automated and automated approaches have been thus developed. The minimum input dataset is a single SAR image, in X, C or L band: a single polarization is generally used, with preference to co-polarization. Using an image pair to perform change detection allows differentiating permanent water from flood, also supporting the discrimination of smooth surfaces and radar shadows. The added value of change detection depends on the selected reference image, which should share the same observation geometry of the flood image, would need to be checked for seasonal effects and for long-lasting flooding. A change detection step (Martinis et al. 2010; Matgen et al. 2011; Long et al. 2014; Amitrano et al. 2018) consists in computing the difference or ratio between the pre-flood and the flood intensity images. As an alternative, the two images can be compared with a graph-based approach, as proposed by Martinis et al. (2010).

As a consequence of the recent abundance of available data, new approaches have been developed to exploit the potential of time series of satellite data. For example, Schlaffer et al. (2015) considered the Envisat archive between 2005 and 2012 to detect flooding, while Martinis et al. (2018) used ESA's Sentinel-1 time series to build a sand exclusion layer, to be used to reduce misclassification of flooding in arid sand-covered areas.

More recently, in particular for flood mapping beneath vegetation coverage and within urban areas, changes in phase and polarization have been shown to be promising and several algorithms have been developed, which also prove useful in mapping open water areas. Irwin et al. (2018) found that dual-polarization methods improve the detection of flooded vegetation, but also of ice and seasonal changes of open water. Olthof and Rainville (2020) concluded that polarimetric information can be of added value when retrieving open water surfaces.

In terms of classification techniques, different methods (or combinations of them) have been proposed. Thresholding aims at separating the two classes of dark water pixels and bright land pixels. Several automated thresholding algorithms have been proposed in the literature, for example by Otsu (1979), Li and Lee (1993) and Yen et al. (1995). Such global thresholding approaches strongly depend on the separability of the two classes, which might vary depending on the portion of image considered and the environmental and weather conditions present at the time of image acquisition, such as high wind or emerging vegetation. To overcome this limitation, different methods have been suggested. The general idea is to perform local thresholding on selected representative areas in the SAR data, for example using split-based approaches (Bovolo and Bruzzone, 2007; Martinis et al. 2009; Twele et al. 2016; Chini et al. 2017; Cao et al. 2017), which show a high probability to comprise adequate portions of the classes "flood" and "non-flood".

Thresholding approaches might result in noisy classification results, given that they do not take into account contextual information. On the contrary, this is possible with both Active Contour Models (ACM, also known as snake) and region growing approaches. ACMs allow the delineation of objects through the evolution of a curve that is driven by an energy function, based on local statistics and regularizing terms. Such models can be initialized by a thresholded region, as done by Heremans et al. (2003), or applied in combination with auxiliary data, like topography data in the work of Mason et al. (2007). With region growing, two steps are needed: after a first selection of seed pixels to generate seed regions, the pixels neighboring the seed region are checked to see if they fulfill the predetermined condition to be added to the seed region itself. This second step is repeated until no more pixels can be added to the seed region. Different approaches can be used to select the seed regions and the predetermined condition to end the region growing process.

For example, Matgen et al. (2011) delineated the seed region with the threshold value at which the empirical and fitted distribution of water start deviating and used as predetermined condition the 99% percentile of the fitted water backscatter distribution. Cao et al. (2018) considered as threshold the mode of the water backscatter distribution as threshold and selected as stopping condition the threshold obtained by the Kittler and Illingworth algorithm (Kittler and Illingworth 1986).

While various rule-based methods for flood mapping based on SAR data have been proposed in the past, convolutional neural networks (CNNs) have seen a rapid development in recent years. CNNs are a branch of artificial neural networks (ANNs) that have been shown to be capable of outperforming traditional image processing techniques in different fields ranging from image classification through object detection to image segmentation. This success can be largely attributed to the generalizing power of CNNs toward spatiotemporal patterns in the data, specifically including contextual signatures, closely mimics human interpretation given enough training data. CNNs have already been successfully applied to various problems in the earth observation domain, including water and flood mapping using either optical or radar data (e.g., Bentivoglio et al. 2021; Wieland and Martinis 2019; Li et al. 2019a, b; Bonafilia et al. 2020; Nemni et al. 2020; Katiyar et al. 2021; Bai et al. 2021; Helleis et al. 2022).

3.2 Vegetated Areas

Detection and extraction of flooded vegetation is of particular importance for two application fields: wetland and flood monitoring. SAR offers the unique opportunity to detect flooded vegetation thanks to its capability to penetrate the vegetation canopy to a certain extent depending on the wavelength and its sensitivity to water underneath the vegetation.

The detectability of partially submerged vegetation is enabled by multiple-bounce effects. SAR backscatter intensity can significantly increase during the presence of water underneath vegetated areas due to the double- or multi-bounce interaction between the specularly reflecting horizontal water surface and vertical structures of the vegetation, such as trunks and stems (Moser et al. 2016; Pulvirenti et al. 2013; Pulvirenti et al. 2011a). Compared to normal water level conditions, this leads to an increased backscatter return to the sensor (Richards et al. 1987; Townsend 2001), as diffuse scattering on the ground reduces the corner reflection effect. The enhancement caused by double-bounce may not always detectable depending on the environmental parameters (e.g., aboveground biomass, vegetation type, phenology of plants, soil moisture, water depth) and sensor characteristics (wavelength, geometric resolution, polarization, incidence angle) (Tsyganskaya et al. 2018a, b). Additionally, backscatter intensities of flooded vegetation can be similar to the backscatter intensities of urban areas and bare soil areas with high-moisture content. This can then result in misclassification (Chapman et al. 2015; Pulvirenti et al. 2016).

The majority of algorithms for the detection of flooded vegetation are intensity-based (Hess and Melack 2003; Evans et al 2010; Arnesen et al. 2013; Cazals et al. 2016; Cian et al. 2018; Olthof and Tolszczuk-Leclerc 2018; Hardy et al. 2019; Grimaldi et al. 2020). Several studies showed the use of InSAR coherence (Refice et al. 2014; Pulvirenti et al. 2016; Chaabani et al. 2018; Brisco et al. 2019) and SAR polarimetry (Plank et al. 2017) to improve the delineation of flooded vegetation. InSAR uses two or more SAR images to generate maps of displacement, using differences in the phase of the waves returning to the sensor. However, such applications are still limited as a consequence of constraining data and computational requirements.

In terms of classification methods, most of the approaches for flooded vegetation mapping are supervised, limiting their transferability and application in real time. For example, manual thresholding has been used by Cazals et al. (2016) and Gallant et al. (2014), while user-defined decision trees (Evans et al. 2010; Arnesen et al. 2013) and machine learning techniques, such as random forest (Chaabani et al. 2018; Tsyganskaya et al. 2018a) and support vector machines (Brisco et al. 2013; Whyte et al. 2018), have also been tested.

Moving to unsupervised approaches, different methods have been proposed, including automated thresholding, fuzzy sets and unsupervised clustering. For example, Cian et al. (2018) suggested an automated thresholding method based on normalized vegetation index. Pulvirenti et al. (2013), Martinis et al. (2015) and Grimaldi et al. (2020) used fuzzy sets to account for various sources of classification uncertainty, while unsupervised clustering has been tested by a number of authors, including, among others, Schlaffer et al. (2016), Irwin et al. (2018), Refice et al. (2020).

3.3 Urban Areas

Flood mapping in urban areas represented a challenge until recently. Urban areas appear very bright in SAR imagery due to the presence of structures that cause double-bounce scattering between streets and buildings. Geometric effects like layover and shadows are also typically very pronounced in urban areas. Additionally, elements like streets might not be wide enough or properly oriented to be visible to the SAR sensor, limiting the ground surface visible to the sensor (Mason et al. 2011, 2012).

Approaches based on intensity change have been applied for a certain time. Mapping flood water in urban area based on the expected low backscatter of open water has been applied by both Giustarini et al. (2013) and Mason et al. (2014), using a region growing approach. Both obtained reasonable results in the less densely built areas but reported underdetection in the more densely built ones. Indeed, flooding close to building enhances the double-bounce backscattering. Such an enhancement has been proven to be detectable by Mason et al. (2014), comparing measured and modeled backscatter. Using intensity change together with topography and contextual information, Pierdicca et al. (2008) mapped flooding in urban area using fuzzy sets. However, it has been shown (Pierdicca et al. 2018) that backscatter in flooded urban areas already approaches saturation in non-flooded conditions.

As a consequence, InSAR coherence is increasingly used in urban flood mapping. For application examples, see, e.g., Chini et al. (2016), Pulvirenti et al. (2016), Kwak et al. (2017), Chaabani et al. (2018), Li et al. (2019a, b).

Recently, the complementarity between SAR intensity and InSAR coherence has been explored. Chini et al. (2019) investigated coherence drops in double-bounce areas, computed based on intensity, coherence time series and information on local incidence angle. On a different note, Li et al. (2019a, b) used a Bayesian network to combine intensity and coherence, followed by a refinement based on conditional random fields (CRF) (Fig. 4). CRFs are a class of statistical modeling methods often applied in pattern recognition and machine learning that can also account for context.
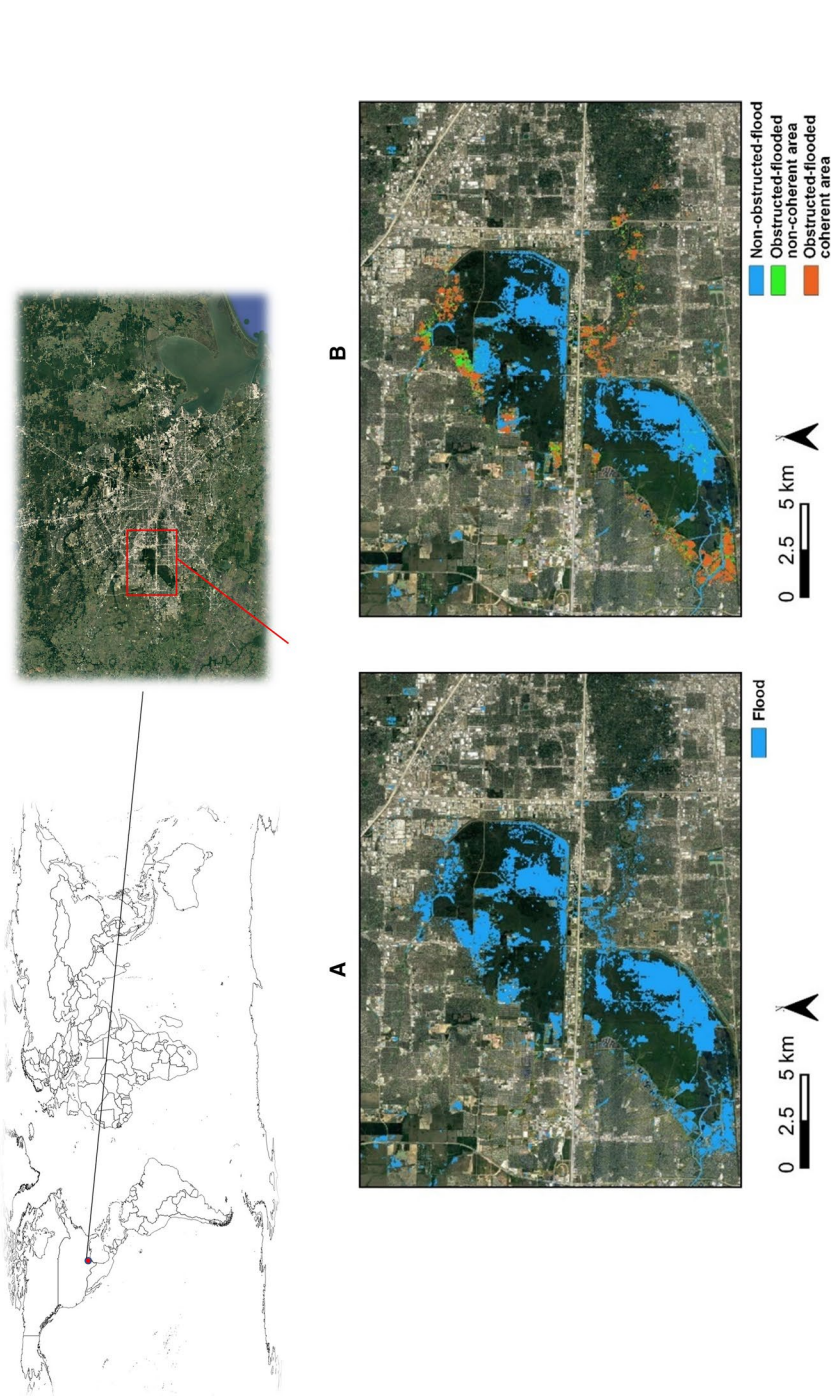
Fig. 4 Flood extent maps of the Houston study area: A. Binary flood extent based on the fusion of intensity σ° and coherence γ; B. Flood category map of A. Modified from . Satellite image display © Google Satellite Layer

4 Altimetry

Satellite altimetry data have great potential for hydrology studies of remote and poorly-gauged catchments and are considered the most promising technology for monitoring the water surface elevation as well as the river discharge from space (International Altimetry Team 2021). Satellite altimeters measure the distance between the satellite and Earth's surface based on the time of travel between signal transmission and sensor reception (Calmant et al. 2008). There are two types of satellite altimeters, the laser and the radar altimeter.

Laser altimetry or LiDAR (Light Detection and Ranging) is best known as airborne sensor technology used for acquisition of high-resolution, high-accuracy topography datasets. Such digital elevation models (DEM) are typically available at a spatial resolution of 50 cm and provide vertical accuracies of 10–20 cm root mean squared error (Mason et al. 2011). Although a costly resource and only available at regional level and in some countries, these DEMs provide the best topographic input data for local highly accurate flood model simulations.

On satellites, such as ICESat-1 and -2, LiDAR has been employed to correct river discharge gauges using local slope of water surface elevations (Hall et al. 2012), to measure river gradients with a high precision (O'Loughlin et al. 2016), and to monitor reservoir and lake water storage (Xu et al. 2021).

However, since satellite missions carrying laser altimetry sensors are still very few in number, satellite radar altimetry is much more frequently used in hydrological studies (Cretaux et al. 2017; Papa et al. 2022), albeit their much lower footprint resolution.

Radar altimeters use several different frequencies depending on mission objectives and they have different spatial (along track sampling and between track distances) and temporal resolution based on the satellite orbit. For example, altimeters on TOPEX/Poseidon and the Jason's family (Jason-1, Jason-2, Jason-3, Sentinel-6A Michael Freilich) operate in Ku and C bands, with a measurement every 10 days and inter-track distance of 315 km at the equator. Altimeters on ERS-1 and ERS-2 (frequency Ku), ENVISAT (frequencies in Ku and S bands) and SARAL/AltiKa (with frequencies in the Ka band), have temporal resolution of 35 days and inter-track of 80 km at the Equator. Altimeters on the Sentinel-3 constellation operate in Ku and C bands, with a temporal resolution of 27 days and inter-track distance of 52 km (if A and B are considered). CryoSat-2, operating on Ku band, has a drifting orbit with a consequent high spatial sampling (7 km) but low temporal resolution (369 days).

The increased availability of all these sensors has encouraged the hydrology community to use satellite altimetry data in river monitoring (see Fig. 5 as an example), addressing numerous applications from water resource management to flood risk mitigation and flood forecasting. In the literature, studies on river monitoring from satellite altimetry have been conducted from large rivers, such as Amazon, Mekong, Congo and Brahmaputra (Da Silva et al. 2010; Chang et al. 2019; Becker et al. 2014; Huang et al. 2018a, b), to small rivers in Indonesia (from 54 to 294 m), in the Ogooué basin (from 180 to 1300 m) or in Italy (from 170 to 450 m) (Sulistioadi et al. 2015; Bogning et al. 2018; Schneider et al. 2018), crossing most climate classifications, from Arctic, temperate and/or tropical rivers (Kouraev et al. 2004; Da Silva et al. 2010; Biancamaria et al. 2017). The wide variety of applications induced to conclude that satellite altimetry is a versatile tool to be used in many environments even if sometimes the quality of water level time series can be compromised by several factors such as the land cover and topography near the channel and channel morphology itself (Maillard et al. 2015).
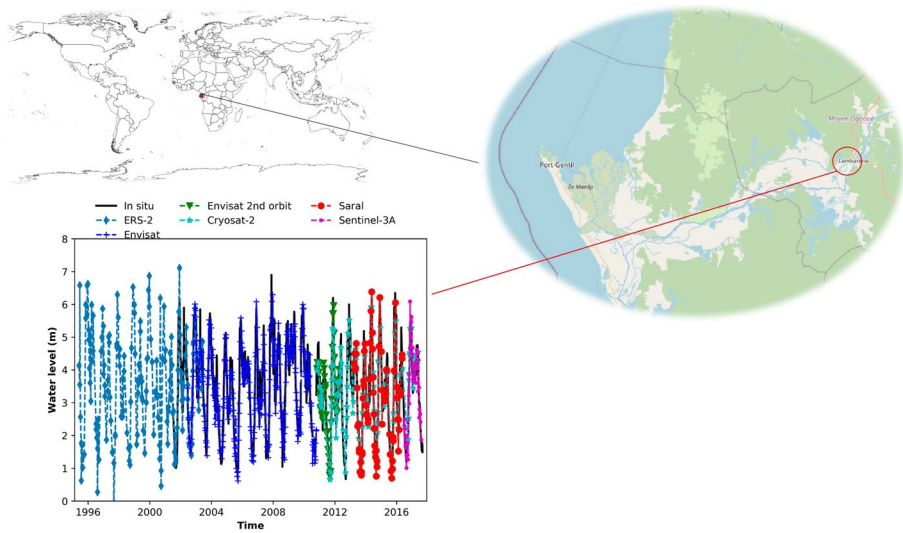
Fig. 5 Example of time series of water level at Lambaréné (Ogooué river basin, located in Gabon, Central Africa) from the in situ gauge record (black continuous line), the multi-mission altimetry-based record (ERS-2 data are represented with diamonds, ENVISAT with blue crosses on its nominal orbit and with green triangles on its second orbit, CryoSat-2 with green–blue stars, SARAL with red circles, Sentinel-3 with purple dots). Modified from Bogning et al. (2018). Map display © OpenStreetMap

Several public online databases exist to obtain altimetry-based time series of water levels over rivers and likes, such as HYDROWEB (https://hydroweb.theia-land.fr/), the Copernicus Global Land Service (https://land.copernicus.eu/global/products/wl), or the Database for Hydrological Time Series of Inland Waters (DAHITI: https://dahiti.dgfi.tum.de/en/products/water-level-altimetry/).

The major drawback in the use of altimetric height is still the temporal resolution (Calmant et al. 2008). However, recent studies overcome the inadequate temporal sampling through the combination of multiple satellite altimetry missions thanks to the development of multi-mission merging approaches (Tourian et al. 2016, 2017; Zakharova et al. 2020; Boergens et al. 2017, 2019; Schwatke et al. 2015). The improved frequency, along with the high accuracy of the altimetry spatial missions (i.e., Sentinel-3 and CryoSat -2), and the recent re-elaboration of past mission focusing on inland water (FDR4ALT, Cryo-TEMPO, HYDROCOASTAL projects funded by ESA) suggest the use of satellite altimetry data for hydrological and hydraulic applications (Birkinshaw et al. 2010; Getirana, 2009; Michailovsky et al. 2013; Domeneghetti et al. 2021; Tarpanelli et al. 2013): altimetry-derived water levels, as traditional in situ river stage measurements, have several uses in the estimation of flooded areas (Sanyal and Lu 2005), and river discharge (Bjerklie et al. 2003; Sichangi et al. 2016; Tarpanelli et al. 2017). As in the traditional procedure, by fitting the satellite measurements of water stage (difference between the altimetry-derived water level and the bottom of the section) with the simultaneous ground measurements of river discharge is possible to establish the functional law, called rating curve. Once the rating curve is fixed, the water levels measured in the future by satellite can be converted directly to discharge (Belloni et al. 2021; Paris et al. 2016; Tourian et al. 2013). The drawback of the procedure is the co-location of the virtual station (the intersection between the river and

the satellite track) with the ground gauged station. Indeed, reliable rating curves are only derived if no significant tributaries or disconnections (dam, reservoirs) are in between.

With the availability of more and more satellite data, traditional approaches were adapted to these new data and empirical formulas, based on the hydraulic relationships between river characteristics, have been revised and adjusted to the use of satellite observations (Bjerklie et al. 2003, 2005; Birkinshaw et al. 2010; Smith and Pavelsky 2008). Water surface width, water level and slope derived by satellite data are used in the empirical relationship to provide estimates of discharge with an average uncertainty of less than 20% (Bjerklie et al. 2003; Sichangi et al. 2016; Tarpanelli et al. 2015). In this context the combination between radar and optical sensors becomes fundamental and the two different operative ways are merged and fused to overcome the limitations or single sensors (Tarpanelli et al. 2019).

5 Passive Microwave Radiometry

The use of passive microwave systems over land surfaces, meaning that surface-emitted wavelengths are measured by the satellite, is, however, difficult given the large angular beams of such systems (Rees 2012), resulting in spatial resolutions as large as 20–100 km. Interpretation of the wide range of materials with many different emissivities is thus rendered nearly impossible. Nevertheless, as the sensor is sensitive to changes in the electric field, very large areas of water, for instance, can be detected but their uncertainties may be large. Successful flood application examples using (passive) microwave radiometry include for example the work by Galantowicz and Picton (2014) for routinely mapping floods, or for operational flood detection as described in De Groeve (2010; see also De Groeve et al. 2006).

The same principle is being applied by the Dartmouth Flood Observatory (DFO: https://floodobservatory.colorado.edu/) to offer a discharge product from microwave brightness temperature. The DFO hosts a database of virtual stations of discharge records from 1998 until present based on an integration of microwave radiometry measurements and global hydrological modeling. The hydrological model (Water Balance Model, WBM (Fekete et al. 2002)) is used for calibrating the microwave signal change (due to changes in surface water area occupying a pixel) to discharge. Specifically, these "River and Reservoir Watch" virtual stations gauge the state of potential large river flooding daily based on changes in the brightness temperature of the passive microwave signal onboard the AMSR-E, TRMM, AMSR-2 and GPM sensors (Brakenridge et al. 2012; http://floodobservatory.colorado.edu/DischargeAccess.html).

6 Integration of EO and Flood Models

Before introducing how EO data is integrated with flood models, it is important to distinguish between a hydrologic and a hydraulic model, or most commonly referred to as flood model. On the one hand, a hydrologic model, in its simpler form, a rainfall-runoff model, is a model that is typically used to output discharge (Q) by simulating parts of the hydrological cycle, and can be in the form of a lumped model or a spatially distributed model. It often requires many parameters with often quite large levels of uncertainties, but can be applied to simulate the evolution of water fluxes, water storage, and potentially associated

chemical and physical properties of the surface and subsurface, largely based on the water balance equation (Eq. 1). On the other hand, a hydraulic, or more commonly referred to as a flood model, is a numerical 1-D or 2-D water flow model based on the Navier–Stokes equation, which is a differential equation that describes the flow of fluids. These models are used to simulate the flow of water through rivers, streams and canals and across adjacent floodplain land. The input variable to these models is typically discharge, and the outputs are typically water depths, flow velocities and water extents.

$$P = Q + AET + GW + DS \tag{1}$$

The long-term water balance equation for a catchment is depicted by Eq. 1, with all terms expressed in mm/year, where P is Precipitation, Q is Runoff, AET is actual evapo-transpiration, GW is exchange with groundwater aquifer and DS is change in soil storage.

Both hydrologic and hydraulic models can be run in historic event mode, nowcast, or forecast mode, with the latter being the most uncertain of course. In the case of flood models, in order to mitigate forecast uncertainties, models have historically been calibrated using in situ hydrometric measurements. However, data from distributed streamflow gauging stations are often not available or, when available, seldom publicly accessible in near-real-time. Moreover, the number of gauging stations worldwide is in decline, and existing coverage is sparse. This has urged developments in complementary directions such as remote sensing and crowdsourcing. Additionally, point measurements of streamflow and water level are not commensurate with the now widely used 2D-models, and therefore cannot effectively constrain model predictions in the floodplain. In recent years, EO data has become a popular and attractive alternative for model implementation, calibration, and validation, and to improve forecast skill through data assimilation.

6.1 Event Calibration and Validation

Real-time two-dimensional inundation patterns of flood events at a high spatial resolution and over large scales is currently possible with aircrafts or satellite imagery. Model simulations of floodplain inundation represent a complement to remote sensing data (see Fig. 6 for an example application). This is important both for re-analysis of past events and for forecast of new inundations.

The previous sections have described in detail that valuable information can be retrieved from flood area and water level. A variety of methods exist to integrate such information with flood models. The most common use of flood area or extent information is for model calibration or validation (see, e.g., Aronica et al. 2002, as one of the classic studies on this topic).

Model calibration can be defined as the process of adjusting model parameters, such as surface roughness or boundary conditions, in order to optimize the fit between model simulations and observations. Validation, or verification, involves comparing model output with observations and using this to deduce model performance. Satellite-derived information is probably most useful to integrate with larger scale flood models (e.g., Neal et al. 2012; Schumann et al. 2013; Wood et al. 2016; Schumann et al. 2016).

6.2 Data Assimilation

Hydrologic and hydraulic models represent powerful tools for simulating streamflow and water levels along the riverbed and in the floodplain. However, input data, model
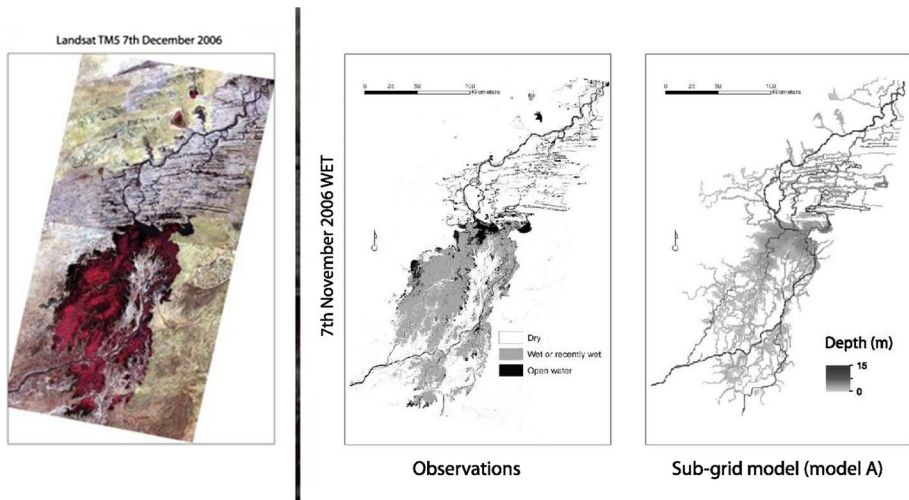
Fig. 6 Comparison between a wet season simulation of the Niger Inland Delta obtained from a 2-D flood inundation model and a Landsat satellite image observation (after Neal et al. 2012)

parameters, initial conditions and model structure represent sources of uncertainty that affect the reliability and accuracy of flood forecasts. Assimilation of satellite-based observations into a flood forecasting model are generally used to reduce such uncertainties. The value that satellite flood maps can add to flood model depends on a number of factors, including image characteristics, regional topography and model uncertainty. In a case where model uncertainty is high, regional topography is complex (i.e., urbanized coastal area) and satellite flood maps are available, assimilation of satellite data can significantly reduce model uncertainty by identifying the "best possible" values of model input variables and/or model parameter sets. However, where oftentimes flood maps can be easily derived, model uncertainty may be relatively low, such as in rural large inland river floodplains. Consequently, not much value from satellites can be added. Nevertheless, where a large number of flood maps are available, model credibility can be increased substantially.

Different variables can be considered for assimilation, including flood extent (Hostache et al. 2018), water levels (García-Pintado et al. 2015) or water surface line derived with the help of DEM, or also directly backscatter values (Cooper et al. 2019). Both real-case studies and synthetic experiments have been analyzed in the literature. Most studies have focused on assimilating synthetic (Matgen et al. 2010; Giustarini et al. 2011; Garambois et al. 2020; Tuozzolo et al. 2019), in situ (Van Wesemael et al. 2019; Ziliani et al. 2019), or remote sensing-derived water levels (RSD-WLs) (Lai and Monnier 2009; Giustarini et al. 2012). The accuracy of the retrieved water levels from remotely sensed flood extents is highly dependent on the DEM accuracy and resolution. Since the DEM is used as an input to the hydraulic model as well as for the retrieval of water levels, the assimilation of satellite-derived water levels may also introduce bias, because the observation and the model are no long independent from each other. In terms of accuracy, this may still be insufficient for application at local scales. Additionally, the spatial flood information is lost during the interpretation of satellite-derived water levels, given that the integration of flood extents and DEMs can only reliably deliver water heights at a few shoreline points.

Given the limitations of water level assimilation, recent studies have focused on developing techniques to directly assimilate flood extent. Variations in modeled or observed flood extents are typically only limited to the boundary of the flooded area. For instance, Cooper et al. (2019) proposed the conversion of modeled binary flood extents into synthetic SAR observations and inter compared the wet and dry backscatter observations at the flood boundary with actual SAR images. While directly utilizing backscatter values reduces the processing time, it discards any information contributed by the addition of texture or coherence, which may reduce uncertainties. Therefore, Hostache et al. (2018) proposed the assimilation of probabilistic flood maps from SAR images in their pioneering study whereby forecasts were updated through direct flood extent comparisons. More recently, Dasgupta et al. (2021) proposed a novel model-data integration method, sensitive to slight variations in the flooded area, and verified its performance through synthetic experiments. At each time step shared information between the model predicted and the observed flooded area was quantified and used to combine their information content, obtaining persistent improvements in predictions of flood extent, depth, and velocity.

In terms of algorithms, the Particle Filter, the Ensemble Kalman Filter and the 4D-Variational technique are the most widely used in hydrology (Dasgupta, et al. 2021). In spite of its popularity in hydrological data assimilation literature, one of the key limitations of the EnKF is the assumption of Gaussianity for model and observation errors. As this assumption does not hold for assimilation of SAR-derived flood observations, some studies have recommended the use of a particle filter framework. A particle filter uses a set of samples to represent the posterior distribution of a stochastic process given the noisy and/or partial observations.

6.3 Improving Simulations and Forecasts

For hydraulic models, the comparison of the several configurations (in situ stations only, satellite altimetry data only, and a combination of in situ and satellite data) showed that the integration of both in situ and radar altimetry data fosters the trustworthiness and reliability of the hydraulic model (Domeneghetti et al. 2014). Among the various applications of altimetry for hydraulic modeling, interesting results are derived by the use of CryoSat-2 satellite data. The small cross-sectional distance of CryoSat-2 tracks ensures distributed observations almost continuously along the river providing added value to the definition of hydrodynamic modeling parameters (i.e., calibration of the roughness coefficient) even in a widely monitored rivers, where ground stations are typically located at longer distances (i.e., 40 km vs 7 km of CryoSat-2). The study by Schneider et al. (2018) demonstrated that high spatial resolution is more important than temporal resolution for calibrating parameters of large-scale river models. Despite the high performance, large uncertainties characterize the modeling due to errors in the model structure, forcing data, parameterization, and initial conditions. Data assimilation of satellite altimetry observations, by updating the model state using independent observations, enables to reduce the uncertainty into the hydrological/hydraulic models (Andreadis et al. 2007; Getirana et al. 2009; Paiva and Collischonn 2013; Michailovsky et al. 2012, 2013).

An important application is represented by the flood forecasting models. Altimetry (and more in general satellite data), if combined with weather, hydrological, and hydrodynamic forecast methods, can mitigate the negative effects of a flood. Among the examples of flood forecasting available in the literature, Hirpa et al. (2013), Tarpanelli et al. (2017)

and Biancamaria et al. (2011) are valuable contributions for describing the use of satellite altimetry for forecasting activities.

In this context, the first satellite mission dedicated to hydrology is planned for launch in 2022. The Surface Water Ocean Topography (SWOT, https://swot.jpl.nasa.gov/) mission (Biancamaria et al. 2016) would be the first global survey of Earth's surface water, observe the fine details of the ocean's surface topography, and measure how water bodies change over time. Its single-pass interferometer will measure water levels and water surface slopes of all main rivers, lakes, and reservoirs, larger than 50–100 m in width. Orbital repeat visits will depend on location and data latency of some science products of more than a month may not lend itself to operational applications, but it will be the first SAR mission that is continuously "on" and will therefore ensure that every place in the satellite coverage is continuously monitored. These novel data are of unprecedented value for monitoring hydrological processes and for updating NWP-, flood-, rainfall-runoff models through data assimilation, or for updating initial conditions in hydrological and hydraulic models.

7 Some New Developments

Artificial Intelligence (AI) and Machine Learning (ML) became the buzz words over the last five years. In almost every industry, people are looking for ways to automate the ways business is done. Reduce the manual labor, increase efficiency, reduce errors and increase the impact of recorded, make the leap forward with the available data. How can we see more, know more with this much 'observed'? Can we teach the machines to see the intricate details of existing data to give us better glimpse of the full picture? Looks like the answer is yes.

With technology getting better and better each day, ML is finding its use cases in insurance industry, specifically on flood risk. Flood risk, being one of the most complicated natural perils we are dealing with, and the most fragmented 'observed' data we have, is the ideal candidate to use AI to improve the understanding.

So far, we have seen AI applications in exposure datasets, satellite imagery, terrain data corrections, near-real-time flood forecasting and even being trialed onboard cubesats for rapid disaster response assistance and other services. The latter application has been developed by a group of researchers that participated in the Frontier Development Lab (FDL) challenge in 2019. The FDL is an artificial intelligence research accelerator for space science (https://frontierdevelopmentlab.org/; https://fdleurope.org/). It is an 8-week space challenge sprint supported by NASA and ESA, along with associated partners. The challenge sprint addresses a number of "hot topic" problem areas and works on solutions based on the newest advances in AI/ML methods, space exploration, and Earth Observation. In the particular challenge in 2019 supported by ESA, the FDL team examined the current limitations related to timely flood map production and delivery. As a solution, the researchers created and curated a unique living database of flood events based on EO data for training a ML model that is light enough to be deployed on a Graphics Processing Unit (GPU) chipset onboard a (series of) CubeSat(s) (Mateo-Garcia et al. 2021). The goal is to rapidly detect and map flooded areas all around the globe thereby eliminating the latency in satellite image delivery. The ML model called *WorldFloods* (Fig. 7) is now being trialed in orbit as part of an experimental flight project. If successful and when operationally deployed in a not-so-distant future, WorldFloods could become game-changing for a

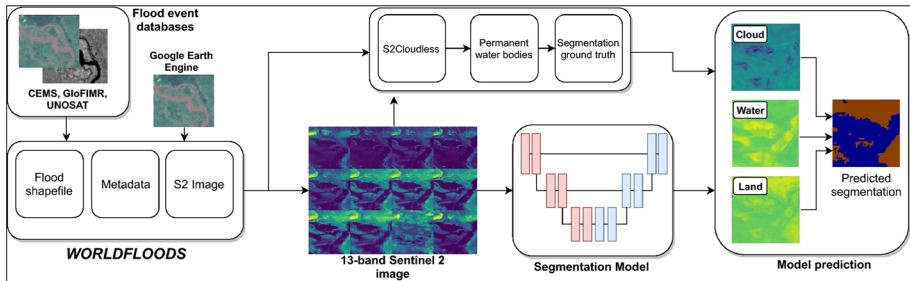**Fig. 7** Overview of the model training pipeline used in this work. Note that WorldFloods provides images from S2, but reference flood extent maps may have been labeled from other sources, such as radar satellites (taken from Mateo-Garcia et al. 2021)

number of sectors, including disaster response, the reinsurance and insurance industry, and, more generally speaking, water resources management.

Another interesting flood mapping application making use of the latest advances in ML/ AI is an ESA-supported project called *FloodSENS* (https://incubed.phi.esa.int/portfolio/ floodsens/). FloodSENS develops a ML-based software application that will be deployed on an online EO cloud-computing platform to rapidly reconstruct flooded area under cloud cover in optical satellite images. This is achieved by training the ML algorithm using relevant auxiliary geospatial datasets such as digital elevation models and water flow grids as well as high-resolution and high-cadence flood labels from drones and very high-resolution commercial satellite imagery. When operationally deployed on the online EO processing platform WASDI (https://www.wasdi.net), the trained model would only use free lower resolution satellite imagery and globally available auxiliary datasets to estimate flooded area under clouds. The application can be run on an event basis or using an archive of flood images. The resulting flood maps would massively increase the information available during a high-impact flood event and also in terms of historical flood observations, allowing us to build better global flood risk indicators.

Another interesting new development is the provision of an operational and freely-available near-real-time Global Flood Monitoring (GFM) product based on the systematic stream of Sentinel-1A/B data for the Copernicus Emergency Management Service (CEMS) of the European Commission (Salamon et al. 2021) within less than eight hours after image acquisition. The flood product is derived by an ensemble approach combining the results of three independently developed flood mapping approaches of Chini et al. (2019), Martinis et al. (2015), and Bauer-Marschallinger et al. (2021), which is integrated into the Global Flood Alert (GloFAS) System (https://www.globalfloods.eu/).

8 Conclusions

This article reviewed the utility of satellite remote sensing, popularly referred to as Earth Observation (EO), to map and monitor floods and its integration with flood modeling approaches. Many of the existing and future satellite missions and airborne platforms provide rich data with great potential for enhanced monitoring, measuring, and mapping of floods, improving hydraulic models through new data assimilation techniques and

parameter scaling behavior, and ultimately for an exploration of the ways in which new data sources may reduce uncertainty in flood predictions.

This has led not only to a better understanding of flood processes at various spatial and temporal scales and better flood forecasts, but also to global initiatives and applications that utilize and promote remote sensing for improved decision-making activities.

With the recent advances in the use of machine learning models and interoperability between models and data, the global user and research communities are entering an era of ever-increasing opportunities but also many new challenges to solve along the way.

Declarations

References

Amitrano D, Di Martino G, Iodice A, Riccio D, Ruello G (2018) Unsupervised rapid flood mapping using sentinel-1 GRD SAR Images. IEEE Trans Geosci Remote Sens 56(6):3290–3299. https://doi.org/10.1109/TGRS.2018.2797536

Andreadis KM, Clark EA, Lettenmaier DP, Alsdorf DE (2007) Prospects for river discharge and depth estimation through assimilation of swath-altimetry into a raster-based hydrodynamics model. Geophys Res Lett. https://doi.org/10.1029/2007GL029721

Arnesen AS et al (2013) Monitoring flood extent in the lower amazon river floodplain using alos/palsar scansar images. Remote Sens Environ 130:51–61. https://doi.org/10.1016/j.rse.2012.10.035

Aronica G, Bates PD, Horritt MS (2002) Assessing the uncertainty in distributed model predictions using observed binary pattern information within GLUE. Hydrol Process 16:2001–2016. https://doi.org/10.1002/hyp.398

Bai Y et al (2021) Enhancement of detecting permanent water and temporary water in flood disasters by fusing sentinel-1 and sentinel-2 imagery using deep learning algorithms: demonstration of Sen1Floods11 benchmark datasets. Remote Sens 13(11):2220. https://doi.org/10.3390/rs13112220

Bauer-Marschallinger B, Cao S, Wagner W, Navacchi C, Tupas ME, Roth F, Pfeil I, Freeman V (2021, in preparation) Satellite-based flood mapping through bayesian inference from sentinel-1 SAR Datacube

Becker M, Da Silva JS, Calmant S, Robinet V, Linguet L, Seyler F (2014) Water level fluctuations in the Congo basin derived from ENVISAT satellite altimetry. Remote Sensing 6(10):9340–9358. https://doi.org/10.3390/rs6109340

Belloni R, Camici S, Tarpanelli A (2021) Towards the continuous monitoring of the extreme events through satellite radar altimetry observations. J Hydrol. https://doi.org/10.1016/j.jhydrol.2021.126870)

Bentivoglio R, Isufi E, Jonkman SN, Taormina R (2021) Deep learning methods for flood mapping: a review of existing applications and future research directions. Hydrol Earth Syst Sci Discuss. https://doi.org/10.5194/hess-2021-614%0A

Biancamaria S, Frappart F, Leleu AS, Marieu V, Blumstein D, Desjonquères JD (2017) Satellite radar altimetry water elevations performance over a 200 m wide river: evaluation over the Garonne River. Adv Space Res 59(1):128–146. https://doi.org/10.1016/j.asr.2016.10.008

Biancamaria S, Hossain F, Lettenmaier DP (2011) Forecasting transboundary river water elevations from space. Geophys Res Lett. https://doi.org/10.1029/2011GL047290

Biancamaria S, Lettenmaier DP, Pavelsky TM (2016) The SWOT mission and its capabilities for land hydrology. In: Cazenave A, Champollion N, Benveniste J, Chen J (eds) Remote sensing and water resources. Space Sciences Series of ISSI, vol 55. Springer, Cham. https://doi.org/10.1007/978-3-319-32449-4_6

Birkinshaw SJ, O'Donnell GM, Moore P, Kilsby CG, Fowler HJ, Berry PAM (2010) Using satellite altimetry data to augment flow estimation techniques on the Mekong River. Hydrol Process 24:3811–3825. https://doi.org/10.1002/hyp.7811

Bjerklie DM, Dingman SL, Vorosmarty CJ, Bolster CH, Congalton RG (2003) Evaluating the potential for measuring river discharge from space. J Hydrol 278:17–38. https://doi.org/10.1016/S0022-1694(03)00129-X

Bjerklie DM, Moller D, Smith LC, Dingman SL (2005) Estimating discharge in rivers using remotely sensed hydraulic information. J Hydrol 309(1–4):191–209. https://doi.org/10.1016/j.jhydrol.2004.11.022

Boergens E, Buhl S, Dettmering D, Klüppelberg C, Seitz F (2017) Combination of multi-mission altimetry data along the Mekong River with spatio-temporal kriging. J Geod 91(5):519–534. https://doi.org/10.1007/s00190-016-0980-z

Boergens E, Dettmering D, Seitz F (2019) Observing water level extremes in the Mekong River Basin: the benefit of long-repeat orbit missions in a multi-mission satellite altimetry approach. J Hydrol 570:463–472. https://doi.org/10.1016/j.jhydrol.2018.12.041

Bogning S, Frappart F, Blarel F, Niño F, Mahé G, Bricquet J-P, Seyler F, Onguéné R, Etamé J, Paiz M-C, Braun J-J (2018) Monitoring water levels and discharges using radar altimetry in an ungauged river basin: the case of the ogooué. Remote Sensing 10(2):350. https://doi.org/10.3390/rs10020350

Bonafilia D, Tellman B, Anderson T, Issenberg E (2020) Sen1Floods11: a georeferenced dataset to train and test deep learning flood algorithms for Sentinel-1. In: 2020 IEEE/CVF conference on computer vision and pattern recognition workshops (CVPRW), Seattle, WA, USA, 2020, pp 835–845. https://doi.org/10.1109/CVPRW50498.2020.00113.

Bovolo F, Bruzzone L (2007) A split-based approach to unsupervised change detection in large-size multitemporal images: application to tsunami-damage assessment. IEEE Trans Geosci Remote Sens 45(6):1658–1670. https://doi.org/10.1109/TGRS.2007.895835

Brakenridge RG, Cohen S, Kettner AJ, De Groeve T, Nghiem SV, Syvitski JPM, Fekete BM (2012) Calibration of satellite measurements of river discharge using a global hydrology model. J Hydrol. https://doi.org/10.1016/j.jhydrol.2012.09.035

Brisco B, Li K, Tedford B, Charbonneau F, Yun S, Murnaghan K (2013) Compact polarimetry assessment for rice and wetland mapping. Int J Remote Sens 34(6):1949–1964. https://doi.org/10.1080/01431161.2012.730156

Brisco B, Shelat Y, Murnaghan K, Montgomery J, Fuss C, Olthof I, Hopkinson C, Deschamps A, Poncos V (2019) Evaluation of C-Band SAR for identification of flooded vegetation in emergency response products. Can J Remote Sens 45(1):73–87. https://doi.org/10.1080/07038992.2019.1612236

Calmant S, Seyler F, Cretaux JF (2008) Monitoring continental surface waters by satellite altimetry. Surv Geophys 29:247–269. https://doi.org/10.1007/s10712-008-9051-1

Cao W, Twele A, Plank S, Martinis S (2018) A three-class change detection methodology for SAR-data based on hypothesis testing and Markov Random field modelling. Int J Remote Sens 39(2):488–504. https://doi.org/10.1080/01431161.2017.1384590

Cao W, Plank S, Martinis S (2017) Automatic SAR-based FLOOD DETECTION USING HIERarchical tile-ranking thresholding and fuzzy logic. IGARSS 2017, Fort Worth, USA, 23.-28.07.2017, https://doi.org/10.1109/IGARSS.2017.8128301.

Cazals C, Rapinel S, Frison P-L, Bonis A, Mercier G, Mallet C, Corgne S, Rudant J-P (2016) Mapping and characterization of hydrological dynamics in a coastal marsh using high temporal resolution Sentinel-1A images. Remote Sens 8:570. https://doi.org/10.3390/rs8070570

Chaabani C, Chini M, Abdelfattah R, Hostache R, Chokmani K (2018) Flood mapping in a complex environment using bistatic TanDEM-X/TerraSAR-X InSAR coherence. Remote Sens 10(12):1873. https://doi.org/10.3390/rs10121873

Chang CH, Lee H, Hossain F, Basnayake S, Jayasinghe S, Chishtie F (2019) A model-aided satellite-altimetry-based flood forecasting system for the Mekong River. Environ Model Softw 112:112–127. https://doi.org/10.1016/j.envsoft.2018.11.017

Chapman B, McDonald K, Shimada M, Rosenqvist A, Schroeder R, Hess L (2015) Mapping regional inundation with spaceborne L-Band SAR. Remote Sensing 7(5):5440–5470. https://doi.org/10.3390/rs70505440

Chini M, Hostache R, Giustarini L, Matgen P (2017) A Hierarchical Split-Based Approach for parametric thresholding of SAR images: flood inundation as a test case. IEEE Trans Geosci Remote Sens 55(12):6975–6988. https://doi.org/10.1109/TGRS.2017.2737664

Chini M, Papastergios A, Pulvirenti L, Pierdicca N, Matgen P, Parcharidis I (2016) SAR coherence and polarimetric information for improving flood mapping. IEEE Int Geosci Remote Sensing Symp 2016:7577–7580. https://doi.org/10.1109/IGARSS.2016.7730976

Chini M, Pelich R, Pulvirenti L, Pierdicca N, Hostache R, Matgen P (2019) Sentinel-1 InSAR coherence to detect floodwater in urban areas: Houston and hurricane Harvey as a test Case. Remote Sens 11:107. https://doi.org/10.3390/rs11020107

Cian F, Marconcini M, Ceccato P (2018) Normalized difference flood index for rapid flood mapping: taking advantage of EO big data. Remote Sensing Environ 209:712–730. https://doi.org/10.1016/j.rse.2018.03.006

Cooper ES, Dance SL, García-Pintado J, Nichols NK, Smith PJ (2019) Observation operators for assimilation of satellite observations in fluvial inundation forecasting. Hydrol Earth Syst Sci 23:2541–2559. https://doi.org/10.5194/hess-23-2541-2019

Copernicus (2021) Flooding in Europe. Online article available here, Accessed on 11/07/2022.

Cretaux J, Nielsen K, Frappart F, Papa F, Calmant S, Benveniste J (2017) Hydrological applications of satellite altimetry: rivers, Lakes, Man-Made Reservoirs. Inundated Areas. https://doi.org/10.1201/9781315151779-14

Currey DT (1977) Identifying flood water movement. Remote Sens Environ 6(1):51–61. https://doi.org/10.1016/0034-4257(77)90019-0

Da Silva JS, Calmant S, Seyler F, Rotunno Filho OC, Cochonneau G, Mansur WJ (2010) Water levels in the Amazon basin derived from the ERS 2 and ENVISAT radar altimetry missions. Remote Sens Environ 114(10):2160–2181. https://doi.org/10.1016/j.rse.2010.04.020

Dasgupta A, Hostache R, Ramsankaran R, Grimaldi S, Matgen P, Chini, M., Pauwels VRN, Walker JP (2021) Earth observation and hydraulic data assimilation for improved flood inundation forecasting. In Earth observation for flood applications, pp 255–294. Elsevier. https://doi.org/10.1016/B978-0-12-819412-6.00012-2

De Groeve T, Kugler Z, Brakenridge GR (2006) Near real time flood alerting for the global disaster alert and coordination system. In: Van De Walle B, Burghardt P, Nieuwenhuis C (eds) Proceedings ISCRAM2007. ISCRAM, Newark, pp 33–39

De Groeve T (2010) Flood monitoring and mapping using passive microwave remote sensing in Namibia. Geomat Nat Haz Risk 1(1):19–35. https://doi.org/10.1080/19475701003648085

Deutsch M, Ruggles FH (1978) Hydrological applications of Landsat imagery used in study of 1973 Indus River flood Pakistan. Water Resour Bull 14(2):261–274. https://doi.org/10.1111/j.1752-1688.1978.tb02165.x

Di Mauro C, Hostache R, Matgen P, Pelich R, Chini M, van Leeuwen PJ, Nichols N, Blöschl G (2021) Assimilation of probabilistic flood maps from SAR data into a coupled hydrologic–hydraulic forecasting model: a proof of concept. Hydrol Earth Syst Sci 25:4081–4097. https://doi.org/10.5194/hess-25-4081-2021

Domeneghetti A, Molari G, Tourian MJ, Tarpanelli A, Behnia S, Moramarco T, Sneeuw N, Brath A (2021) Testing the use of single- and multi-mission satellite altimetry for the calibration of hydraulic models. Adv Water Res 151:103887. https://doi.org/10.1016/j.advwatres.2021.103887

Domeneghetti A, Tarpanelli A, Brocca L, Barbetta S, Moramarco T, Castellarin A, Brath A (2014) The use of remote sensing-derived water surface data for hydraulic model calibration. Remote Sens Environ 149:130–141. https://doi.org/10.1016/j.rse.2014.04.007

Evans TL et al (2010) Using ALOS/PALSAR and RADARSAT-2 to map land cover and seasonal inundation in the Brazilian pantanal. IEEE J Select Topics Appl Earth Observ Remote Sens 3:560–575. https://doi.org/10.1109/JSTARS.2010.2089042

Fekete BM, Vöröosmarty CJ, Grabs W (2002) High-resolution fields of global runoff combining observed river discharge and simulated water balances. Global Biogeochem Cycles. https://doi.org/10.1029/1999GB001254

Galantowicz JF, Picton J (2014) Flood extent depiction by physical downscaling of flooded fraction estimates from microwave remote sensing. In: 2014 IEEE geoscience and remote sensing symposium, Quebec City, QC, 2014, pp 3854–3857. https://doi.org/10.1109/IGARSS.2014.6947325

Gallant AL, Kaya SG, White L, Brisco B, Roth MF, Sadinski W, Rover J (2014) Detecting emergence, growth, and senescence of wetland vegetation with polarimetric synthetic aperture radar (SAR) Data. Water 6(3):694–722. https://doi.org/10.3390/w6030694

Garambois P-A, Larnier K, Monnier J, Finaud-Guyot P, Verley J, Montazem A, Calmant S (2020) Variational inference of effective channel and ungauged anabranching river discharge from multi-satellite water heights of different spatial sparsity. J Hydrol 581:124–409

Garcia-Pintado J et al (2015) Satellite-supported food forecasting in river networks: a real case study. J Hydrol 523:706–724. https://doi.org/10.1016/j.jhydrol.2015.01.084

Getirana ACV, Bonnet MP, Calmant S, Roux E, Rotunno OC, Mansur WJ (2009) Hydrological monitoring of poorly gauged basins based on rainfall-runoff modeling and spatial altimetry. J Hydrol 379:205–219. https://doi.org/10.1016/j.jhydrol.2009.09.049

Giustarini L, Hostache R, Matgen P, Schumann GJP, Bates PD, Mason DC (2013) A change detection approach to flood mapping in Urban areas using TerraSAR-X. IEEE Trans Geosci Remote Sens 51(4):2417–2430. https://doi.org/10.1109/TGRS.2012.2210901

Giustarini L, Matgen P, Hostache R, Montanari M, Plaza D, Pauwels VRN, De Lannoy GJM, De Keyser R, Pfister L, Hoffmann L, Savenije HHG (2011) Assimilating SAR-derived water level data into a hydraulic model: a case study. Hydrol Earth Syst Sci 15:2349–2365. https://doi.org/10.5194/hess-15-2349-2011

Giustarini L, Matgen P, Hostache R, Dostert J (2012) From SAR-derived flood mapping to water level data assimilation into hydraulic models. In: Proceedings of SPIE 8531, remote sensing for agriculture, ecosystems, and hydrology XIV: 85310U. https://doi.org/10.1117/12.974655. Accessed 19 Oct 2012.

Grimaldi S, Xu J, Li Y, Pauwels VRN, Walker JP (2020) Flood mapping under vegetation using single SAR acquisitions. Remote Sens Environ. https://doi.org/10.1016/j.rse.2019.111582

Hall AC, Schumann GJ-P, Bamber JL, Bates PD, Trigg MA (2012) Geodetic corrections to Amazon River water level gauges using ICESat altimetry. Water Resour Res. https://doi.org/10.1029/2011WR010895

Hardy A, Ettritch G, Cross DE, Bunting P, Liywalii F, Sakala J, Silumesii A, Singini D, Smith M, Willis T, Thomas CJ (2019) Automatic detection of open and vegetated water bodies using sentinel 1 to map african malaria vector mosquito breeding habitats. Remote Sens 11:593. https://doi.org/10.3390/rs11050593

Helleis M, Wieland M, Krullikowski C, Martinis S, Plank S (2022) Sentinel-1-based water and flood mapping: benchmarking convolutional neural networks against an operational rule-based processing chain. IEEE J Select Top Appl Earth Observ Remote Sens 15:2023–2036. https://doi.org/10.1109/JSTARS.2022.3152127

Heremans R, et al (2003) Automatic detection of flooded areas on ENVISAT/ASAR images using an object-oriented classification technique and an active contour algorithm. In: Proceedings of international conference on recent advances in space technologies. RAST '03. pp 311–316. https://doi.org/10.1109/RAST.2003.1303926

Hess LL, Melack JM (2003) Remote sensing of vegetation and flooding on Magela Creek Floodplain (Northern Territory, Australia) with the SIR-C synthetic aperture radar. Hydrobiologia 500:65–82. https://doi.org/10.1023/A:1024665017985

Hirpa FA, Hopson TM, De Groeve T, Brakenridge GR, Gebremichael M, Restrepo PJ (2013) Upstream satellite remote sensing for river discharge forecasting: application to major rivers in South Asia. Remote Sens Environ 131:140–151. https://doi.org/10.1016/j.rse.2012.11.013

Hostache R, Chini M, Giustarini L, Neal J, Kavetski D, Wood M, Corato G, Pelich R-M, Matgen P (2018) Near-real-time assimilation of SAR-derived flood maps for improving flood forecasts. Water Resour Res. https://doi.org/10.1029/2017WR022205

Huang C, Chen Y, Zhang S, Wu J (2018a) Detecting, extracting, and monitoring surface water from space using optical sensors: a review. Rev Geophys 56(2):333–360. https://doi.org/10.1029/2018RG000598

Huang Q, Long D, Du M, Zeng C, Li X, Hou A, Hong Y (2018b) An improved approach to monitoring Brahmaputra River water levels using retracked altimetry data. Remote Sens Environ 211:112–128. https://doi.org/10.1016/j.rse.2018.04.018

International Altimetry Team (2021) Altimetry for the future: Building on 25 years of progress. Adv Space Res 68(2):319–363. https://doi.org/10.1016/j.asr.2021.01.022

Irwin K, Braun A, Fotopoulos G, Roth A, Wessel B (2018) Assessing single-polarization and dual-polarization TerraSAR-X data for surface water monitoring. Remote Sens 10:949. https://doi.org/10.3390/rs10060949

Katiyar V, Tamkuan N, Nagai M (2021) Near-Real-time flood mapping using off-the-shelf models with SAR imagery and deep learning. Remote Sens 13(12):2334. https://doi.org/10.3390/rs13122334

Kittler J, Illingworth J (1986) Minimum error thresholding. Pattern Recogn 19(1):41–47. https://doi.org/10.1016/0031-3203(86)90030-0

Kouraev AV, Zakharova EA, Samain O, Mognard NM, Cazenave A (2004) Ob'river discharge from TOPEX/Poseidon satellite altimetry (1992–2002). Remote Sens Environ 93(1–2):238–245. https://doi.org/10.1016/j.rse.2004.07.007

Kwak Y, Yun S, Iwami Y (2017) A new approach for rapid urban flood mapping using ALOS-2/PALSAR-2 in 2015 Kinu River Flood, Japan. IEEE Int Geosci Remote Sensing Symp 2017:1880–1883. https://doi.org/10.1109/IGARSS.2017.8127344

Lai X, Monnier J (2009) Assimilation of spatially distributed water levels into a shallow-water flood model. Part I: Mathematical method and test case. J Hydrol 377(1–2):1–11

Li CH, Lee CK (1993) Minimum cross entropy thresholding. Pattern Recogn 26(4):617–625. https://doi.org/10.1016/0031-3203(93)90115-D

Li Y, Martinis S, Wieland M (2019a) Urban flood mapping with an active self-learning convolutional neural network based on TerraSAR-X intensity and interferometric coherence. ISPRS J Photogramm Remote Sens 152:178–191. https://doi.org/10.1016/j.isprsjprs.2019.04.014

Li Y, Martinis S, Wieland M, Schlaffer S, Natsuaki R (2019b) Urban flood mapping using SAR intensity and interferometric coherence via bayesian network fusion. Remote Sens 11:2231. https://doi.org/10.3390/rs11192231

Li S, Sun D, Goldberg MD, Sjoberg B, Santek D, Hoffman JP, DeWeese M, Restrepo P, Lindsey S, Holloway E (2018) Automatic near real-time flood detection using Suomi-NPP/VIIRS data. Remote Sens Environ 204:672–689. https://doi.org/10.1016/j.rse.2017.09.032

Long S, Fatoyinbo TE, Policelli F (2014) Flood extent mapping for Namibia using change detection and thresholding with SAR. Environ Res Lett 9(3):9. https://doi.org/10.1088/1748-9326/9/3/035002

Maillard P, Bercher N, Calmant S (2015) New processing approaches on the retrieval of water levels in Envisat and SARAL radar altimetry over rivers: a case study of the São Francisco River. Brazil Remote Sens Environ 154:226241. https://doi.org/10.1016/j.rse.2014.09.027

Marcus WA, Fonstad MA (2008) Optical remote mapping of rivers at sub-meter resolutions and watershed extents. Earth Surf Proc Land 33:4–24. https://doi.org/10.1002/esp.1637

Martinis S, Plank S, Ćwik K (2018) The Use of Sentinel-1 time-series data to improve flood monitoring in arid areas. Remote Sens 10:583. https://doi.org/10.3390/rs10040583

Martinis S, Twele A, Kersten J (2015) A fully automated TerraSAR-X based flood service. ISPRS J Photogramm Remote Sens 104:203–212. https://doi.org/10.1016/j.isprsjprs.2014.07.014

Martinis S, Twele A, Voigt S (2009) Towards operational near real-time flood detection using a split-based automatic thresholding procedure on high resolution TerraSAR-X data. Nat Hazard 9:303–314. https://doi.org/10.5194/nhess-9-303-2009

Martinis S (2010): Automatic near real-time flood detection in high resolution X-band synthetic aperture radar satellite data using context-based classification on irregular graphs. Dissertation, LMU München: Faculty of Geosciences https://edoc.ub.uni-muenchen.de/12373/1/Martinis_Sandro.pdf

Mason DC, Davenport IJ, Neal JC, Schumann GJ, Bates PD (2012) Near real-time flood detection in urban and rural areas using high-resolution synthetic aperture radar images. IEEE Trans Geosci Remote Sens 50(8):3041–3052. https://doi.org/10.1109/TGRS.2011.2178030

Mason DC, Giustarini L, Garcia-Pintado J, Cloke HL (2014) Detection of flooded urban areas in high resolution Synthetic Aperture Radar images using double scattering. Int J Appl Earth Obs Geoinf 28(2014):150–159. https://doi.org/10.1016/j.jag.2013.12.002

Mason DC, Horritt MS, Dall'Amico JT, Scott TR, Bates PD (2007) Improving river flood extent delineation from synthetic aperture radar using airborne laser altimetry. IEEE Trans Geosci Remote Sens 45(12):3932–3943. https://doi.org/10.1109/TGRS.2007.901032

Mason DC, Schumann GJ-P, Bates PD (2011) Data utilization in flood inundation models. In: Pender G, Faulkner H (eds) Flood risk science and management. Wiley-Blackwell, pp 211–233

Mateo-Garcia G, Veitch-Michaelis J, Smith L et al (2021) Towards global flood mapping onboard low cost satellites with machine learning. Sci Rep 11:7249. https://doi.org/10.1038/s41598-021-86650-z

Matgen P, Hostache R, Schumann G, Pfister L, Hoffmann L, Savenije HHG (2011) Towards an automated SAR-based flood monitoring system: Lessons learned from two case studies. Phys Chem Earth 36(7–8):241–252. https://doi.org/10.1016/j.pce.2010.12.009

Matgen P, Montanari M, Hostache R, Pfister L, Hoffmann L, Plaza D, Pauwels VRN, De Lannoy GJM, De Keyser R, Savenije HHG (2010) Towards the sequential assimilation of SAR-derived water stages into hydraulic models using the Particle Filter: proof of concept. Hydrol Earth Syst Sci 14:1773–1785. https://doi.org/10.5194/hess-14-1773-2010

McFeeters SK (1996) The use of the normalized difference water index (NDWI) in the delineation of open water features. Int J Remote Sens 17:1425–1432. https://doi.org/10.1080/01431169608948714

Michailovsky CI, McEnnis S, Berry PAM, Smith R, Bauer-Gottwein P (2012) River monitoring from satellite radar altimetry in the Zambezi River basin. Hydrol Earth Syst Sci 16(7):2181–2192. https://doi.org/10.5194/hess-16-2181-2012

Michailovsky CI, Milzow C, Bauer-Gottwein P (2013) Assimilation of radar altimetry to a routing model of the Brahmaputra River. Water Resour Res 49:4807–4816. https://doi.org/10.1002/wrcr.20345

Moser L, Schmitt A, Wendleder A, Roth A (2016) Monitoring of the lac bam wetland extent using dual-polarized X-band SAR data. Remote Sensing 8(4):302. https://doi.org/10.3390/rs8040302

Munich Re (2017). Natural catastrophes 2017: analyses, assessments, positions. TOPICS Geo reports, Munich Re Publications, available at www.munichre.com

Munich Re (2022) Hurricanes, cold waves, tornadoes: Weather disasters in USA dominate natural disaster losses in 2021. Report published on 10/01/2022, available here.

Neal JC, Schumann GJ-P, Bates PD (2012) A sub-grid channel model for simulating river hydraulics and floodplain inundation over large and data sparse areas. Water Resour Res. https://doi.org/10.1029/2012WR012514

Nemni E, Bullock J, Belabbes S, Bromley L (2020) Fully convolutional neural network for rapid flood segmentation in synthetic aperture radar imagery. Remote Sensing. https://doi.org/10.3390/rs12162532

O'Loughlin FE, Neal J, Yamazaki D, Bates PD (2016) ICESat-derived inland water surface spot heights. Water Resour Res 52:3276–3284. https://doi.org/10.1002/2015WR018237

Olthof I, Rainville T (2020) Evaluating simulated RADARSAT Constellation Mission (RCM) compact polarimetry for open-water and flooded-vegetation wetland mapping. Remote Sens 12:1476. https://doi.org/10.3390/rs12091476

Olthof I, Tolszczuk-Leclerc S (2018) Comparing Landsat and RADARSAT for current and historical dynamic flood mapping. Remote Sens 10:780. https://doi.org/10.3390/rs10050780

Otsu N (1979) A threshold selection method from gray-level histograms. IEEE Trans Syst Man Cybern 9(1):62–66. https://doi.org/10.1109/TSMC.1979.4310076

Paiva RCD, Collischonn W (2013) Buarque DC Validation of a full hydrodynamic model for large-scale hydrologic modelling in the Amazon. Hydrol Process 27:333–346. https://doi.org/10.1002/hyp.842

Papa F, Crétaux JF, Grippa M et al (2022) Water Resources in Africa under Global Change: Monitoring Surface Waters from Space. Surv Geophys. https://doi.org/10.1007/s10712-022-09700-9

Paris A, Dias de Paiva R, Santos da Silva J, Medeiros Moreira D, Calmant S, Garambois PA (2016) Stage-discharge rating curves based on satellite altimetry and modeled discharge in the Amazon basin. Water Resour Res 52(5):3787–3814. https://doi.org/10.1002/2014WR016618

Pierdicca N, Chini M, Pulvirenti L, Macina F (2008) Integrating physical and topographic information into a fuzzy scheme to map flooded area by SAR. Sensors 8(7):4151–4164. https://doi.org/10.3390/s8074151

Pierdicca N, Pulvirenti L, Chini M (2018) Flood mapping in vegetated and urban areas and other challenges: models and methods. In: Refice A, D'Addabbo A, Capolongo D (eds) Flood monitoring through remote sensing. Springer Remote Sensing/Photogrammetry. Springer, Cham. https://doi.org/10.1007/978-3-319-63959-8_7

Plank S, Jüssi M, Martinis S, Twele A (2017) Mapping of flooded vegetation by means of polarimetric Sentinel-1 and ALOS-2/PALSAR-2 imagery. Int J Remote Sens 38:3831–3850. https://doi.org/10.1080/01431161.2017.1306143

Pulvirenti L et al (2016) Use of SAR data for detecting floodwater in urban and agricultural areas: the role of the interferometric coherence. IEEE Trans Geosci Remote Sens 54(3):1532–1544. https://doi.org/10.1109/TGRS.2015.2482001

Pulvirenti L, Chini M, Pierdicca N, Guerriero L, Ferrazzoli P (2011) Flood monitoring using multi-temporal COSMO-SkyMed data. Image segmentation and signature interpretation. Remote Sens Environ 115(4):990–1002. https://doi.org/10.1016/j.rse.2010.12.002

Pulvirenti L, Pierdicca N, Chini M, Guerriero L (2013) Monitoring flood evolution in vegetated areas using COSMO-SkyMed data: the Tuscany 2009 case study. IEEE J Sel Top Appl Earth Observ Remote Sensing 6(4):1807–1816. https://doi.org/10.1109/JSTARS.2012.2219509

Rees W (2012) Physical principles of remote sensing, 3rd edn. Cambridge University Press, Cambridge. https://doi.org/10.1017/CBO9781139017411

Refice A et al (2014) SAR and InSAR for flood monitoring: examples with COSMO-SkyMed data. IEEE J Select Top Appl Earth Observ Remote Sensing 7(7):2711–2722. https://doi.org/10.1109/JSTARS.2014.2305165

Refice A, Zingaro M, D'Addabbo A, Chini M (2020) "Integrating C- and L-Band SAR Imagery for Detailed Flood Monitoring of Remote Vegetated Areas. Water 12(10):2745. https://doi.org/10.3390/w12102745

Richards JA, Woodgate PW, Skidmore AK (1987) An explanation of enhanced radar backscattering from flooded forests. Int J Remote Sens 8:1093–1100. https://doi.org/10.1080/01431168708954756

Robinove CJ (1978) Interpretation of a Landsat image of an unusual flood phenomenon in Australia. Remote Sens Environ 7(3):219–225. https://doi.org/10.1016/0034-4257(78)90033-0

Salamon P, McCormick N, Reimer C, Clarke T, Bauer-Marschallinger B, Wagner W, Martinis S, Chow C, Böhnke C, Matgen P, Chini M, Hostache R, Molini L, Fiori E, Walli A (2021) The new, systematic global flood monitoring product of the Copernicus Emergency Management Service. IGARSS 2021, Brussels, 2021, https://doi.org/10.1109/IGARSS47720.2021.9554214.

Sanyal J, Lu XX (2005) Remote sensing and GIS-based flood vulnerability assessment of human settlements: a case study of Gangetic West Bengal. India Hydrol Process 19(18):3699–3716. https://doi.org/10.1002/hyp.5852

Schlaffer S, Chini M, Dettmering D, Wagner W (2016) Mapping wetlands in zambia using seasonal backscatter signatures derived from ENVISAT ASAR time series. Remote Sens 8:402. https://doi.org/10.3390/rs8050402

Schlaffer S, Matgen P, Hollaus M, Wagner W (2015) Flood detection from multi-temporal SAR data using harmonic analysis and change detection. Int J Appl Earth Obs Geoinf 38:15–24. https://doi.org/10.1016/j.jag.2014.12.001

Schneider R, Tarpanelli A, Nielsen C, Madsen H, Bauer-Gottwein P (2018) Evaluation of multi-mode CryoSat-2 altimetry data over the Po River against in situ data and a hydrodynamic model. Adv Water Resour 112:17–26. https://doi.org/10.1016/j.advwatres.2017.11.027

Schumann G, Di Baldassarre G, Bates PD (2009) The utility of spaceborne radar to render flood inundation maps based on multialgorithm ensembles. IEEE Trans Geosci Remote Sens 47(8):2801–2807. https://doi.org/10.1109/TGRS.2009.2017937

Schumann GJ-P, Domeneghetti A (2016) Exploiting the proliferation of current and future satellite observations of rivers. Hydrol Process 30(16):2891–2896. https://doi.org/10.1002/hyp.10825

Schumann GJ-P, Neal JC, Voisin N, Andreadis KM, Pappenberger F, Phanthuwongpakdee N, Hall AC, Bates PD (2013) A first large scale flood inundation forecasting model. Water Resour Res 49:6248–6257. https://doi.org/10.1002/wrcr.20521

Schumann GJ-P, Stampoulis D, Smith AM, Sampson CC, Andreadis KM, Neal JC, Bates PD (2016) Rethinking flood hazard at the global scale. Geophys Res Lett 43:10249–10256. https://doi.org/10.1002/2016GL070260

Schwatke C, Dettmering D, Bosch W, Seitz F (2015) DAHITI–an innovative approach for estimating water level time series over inland waters using multi-mission satellite altimetry. Hydrol Earth Syst Sci 19(10):4345–4364. https://doi.org/10.5194/hess-19-4345-2015

Shen X, Wang D, Mao K, Anagnostou E, Hong Y (2019) Inundation extent mapping by synthetic aperture radar: a review. Remote Sens 11:879. https://doi.org/10.3390/rs11070879

Sichangi AW, Wang L, Yang K, Chen D, Wang Z, Li X, Zhou J, Liu W, Kuria D (2016) Estimating continental river basin discharges using multiple remote sensing data sets. Remote Sens Environ 179:36–53. https://doi.org/10.1016/j.rse.2016.03.019

Smith LC, Pavelsky TM (2008) Estimation of river discharge, propagation speed, and hydraulic geometry from space: Lena River. Water Resour Res, Siberia. https://doi.org/10.1029/2007WR006133

Sulistioadi YB, Tseng K-H, Shum CK, Hidayat H, Sumaryono M, Suhardiman A, Setiawan F, Sunarso S (2015) Satellite radar altimetry for monitoring small rivers and lakes in Indonesia. Hydrol Earth Syst Sci 19:341–359. https://doi.org/10.5194/hess-19-341-2015

Swiss Re (2021) Remote sensing technology in claims assessment—lessons learned from the 2021 Australia East Coast floods. Available at: https://www.swissre.com/risk-knowledge/mitigating-climate-risk/remote-sensing-technology-in-claims-assessment.html 23 Sep 2021.

Tarpanelli A, Amarnath G, Brocca L, Massari C, Moramarco T (2017) Discharge estimation and forecasting by MODIS and altimetry data in Niger-Benue River. Remote Sens Environ 195:96–106. https://doi.org/10.1016/j.rse.2017.04.015

Tarpanelli A, Barbetta S, Brocca L, Moramarco T (2013) River discharge estimation by using altimetry data and simplified flood routing modeling. Remote Sens 5(9):4145–4162. https://doi.org/10.3390/rs5094145

Tarpanelli A, Brocca L, Barbetta S, Faruolo M, Lacava T, Moramarco T (2015) Coupling MODIS and radar altimetry data for discharge estimation in poorly gauged river basin. IEEE J SelectTop Appl Earth Observ Remote Sensing 8(1):141–148. https://doi.org/10.1109/JSTARS.2014.2320582

Tarpanelli A, Camici S, Nielsen K, Brocca L, Moramarco T, Benveniste J (2019) Potentials and limitations of Sentinel-3 for river discharge assessment. Adv Space Res 68(2):593–606. https://doi.org/10.1016/j.asr.2019.08.005

The Insurance Journal (2021) Swiss Re Estimates Europe's July Floods to Cost Insurers $12 Billion. Available at: https://www.insurancejournal.com/news/international/2021/10/05/635447.htm, 6 Oct 2021

Tourian MJ, Schwatke C, Sneeuw N (2017) River discharge estimation at daily resolution from satellite altimetry over an entire river basin. J Hydrol 546:230–247. https://doi.org/10.1016/j.jhydrol.2017.01.009

Tourian MJ, Sneeuw N, Bardossy A (2013) A quantile function approach to discharge estimation from satellite altimetry (ENVISAT). Water Resour Res 49(7):4174–4186. https://doi.org/10.1002/wrcr.20348

Tourian MJ, Tarpanelli A, Elmi O, Qin T, Brocca L, Moramarco T, Sneeuw N (2016) Spatiotemporal densification of river water level time series by multimission satellite altimetry. Water Resour Res 52(2):1140–1159. https://doi.org/10.1002/2015WR017654

Townsend PA (2001) Mapping seasonal flooding in forested wetlands using multi-temporal SAR. Photogramm Eng Remote Sens 67:857–864

Tsyganskaya V, Martinis S, Marzahn P, Ludwig R (2018b) SAR-based detection of flooded vegetation—a review of characteristics and approaches. Int J Remote Sens. https://doi.org/10.1080/01431161.2017.1420938

Tsyganskaya V, Martinis S, Marzahn P, Ludwig R (2018a) Detection of temporary flooded vegetation using sentinel-1 time series data. In: Remote sensing, vol 10, No. 8, 1286, https://doi.org/10.3390/rs10081286

Tuozzolo S, Lind G, Overstreet B, Mangano J, Fonstad M, Hagemann M et al (2019) Estimating river discharge with swath altimetry: A proof of concept using AirSWOT observations. Geophys Res Lett 46:1459–1466. https://doi.org/10.1029/2018GL080771

Twele A, Cao W, Plank S, Martinis S (2016) Sentinel-1-based flood mapping: a fully automated processing chain. Int J Remote Sens 37(13):2990–3004. https://doi.org/10.1080/01431161.2016.1192304

Van Wesemael A, Landuyt L, Lievens H, Verhoest NEC (2019) Improving flood inundation forecasts through the assimilation of in situ floodplain water level measurements based on alternative observation network configurations. Adv Water Resour 130:229–243. https://doi.org/10.1016/j.advwatres.2019.05.025

Whyte A, Ferentinos KP, Petropoulos GP (2018) A new synergistic approach for monitoring wetlands using Sentinels -1 and 2 data with object-based machine learning algorithms. Environ Model Softw 104:40–54. https://doi.org/10.1016/j.envsoft.2018.01.023

Wieland M, Martinis S (2019) A modular processing chain for automated flood monitoring from multispectral satellite data. Remote Sensing. https://doi.org/10.3390/rs11192330

Wood M, Hostache R, Neal J, Wagener T, Giustarini L, Chini M, Corato G, Matgen P, Bates P (2016) Calibration of channel depth and friction parameters in the LISFLOOD-FP hydraulic model using medium-resolution SAR data and identifiability techniques. Hydrol Earth Syst Sci 20:4983–4997. https://doi.org/10.5194/hess-20-4983-2016

Xu N, Zheng H, Ma Y, Yang J, Liu X, Wang X (2021) Global Estimation and assessment of monthly lake/reservoir water level changes using ICESat-2 ATL13 products. Remote Sens 13:2744. https://doi.org/10.3390/rs13142744

Yen J-C et al (1995) A new criterion for automatic multilevel thresholding. IEEE Trans Image Process 4(3):370–378. https://doi.org/10.1109/83.366472

Zakharova E, Nielsen K, Kamenev G, Kouraev A (2020) River discharge estimation from radar altimetry: assessment of satellite performance, river scales and methods. J Hydrol 583:124561. https://doi.org/10.1016/j.jhydrol.2020.124561

Ziliani MG, Ghostine R, Ait-El-Fquih B, McCabe MF, Hoteit I (2019) Enhanced flood forecasting through ensemble data assimilation and joint state-parameter estimation. J Hydrol. https://doi.org/10.1016/j.jhydrol.2019.123924